

# Exploring New Physics of Nanoparticle Supercrystals by High Pressure Small Angle X-ray Diffraction

Zhongwu Wang, Ken Finkelstein, and Detlef-M. Smilgies

Cornell High Energy Synchrotron Source, Cornell University

Superlattices built from self-assembled nanoparticles (NPs) combine the size-tuned unique properties of single crystals with the collective properties of newly created (one- two- and three-dimensional) ordered arrays and promise the next generation of devices spanning a variety of applications<sup>1-4</sup>. For example, in nature, a colorless opal is a disordered aggregate of silica particles. When the silica particles are ordered, the opal changes to a color correlated with the size of the self-assembled particles<sup>3</sup>. In the laboratory, several approaches, including templating, soft lithography and supramolecular chemistry, have enabled creation of numerous superlattices comprising NP building blocks<sup>3,5-7</sup>. These NP nanobuilding blocks fall mostly into three types of order displaying variable packing densities and properties: Face-Centered-Cubic (FCC), Hexagonal-Centered-Packing (HCP) and Body-Centered-Cubic (BCC) or Body-Centered Tetragonal (BCT) (Fig. 1)<sup>4</sup>. To facilitate custom engineered applications for NP superlattices requires understanding the structural and mechanical stabilities, inter-NP interaction and tuning mechanisms. In order to explore the structure and dynamic behavior at atomic resolution as NPs evolve into ordered building blocks and are tuned for stable structures and novel properties, we have developed a powerful *in-situ* synchrotron x-ray technique. Our window capable of peeking into the mysterious nanoworld utilizes small and wide angle x-ray diffraction under varying pressure and temperature for the exploration of the new physics and chemistry of NP supercrystals.

Probing a wide spectrum of information of NP superlattice formation covering the atomic scale and the nanoscale requires monitoring x-ray diffraction from NP supercrystals in the small and the wide angle range. The complexity of

measurement increases with application of pressure and involves several key experimental components: a pressure cell with transparent x-ray windows, x-ray energy tuning and position control of a large area detector. The diamond anvil cell (DAC) is certainly the primary option to reach extreme pressure, but strong absorption of low energy x-rays by diamond limits the measurement of small angle x-ray scattering. We circumvent these problems by tuning x-ray energy and sample-to-detector distance. At a wavelength optimized to avoid significant weakening of the scattering signal, we optimize detector position for collection of both first-order small angle and wide angle x-ray diffraction by taking several exposures at different detector positions (but without multiple calibrations of sample-to-detector distance).

Our DAC has a large downstream angular opening that covers the wide angle x-ray diffraction. For a supercrystal sample made up of nanoparticles with known size, we roughly estimate the angle and corresponding position of the first order small angle x-ray diffraction peaks at different x-ray wavelengths, and then tune the x-ray energy to the optimum value at one intermediate

sample-to-detector distance. After a quick check of the diffraction image, we move the detector to a long distance from the sample, enabling observation of small angle x-ray diffraction rings. After one calibration of sample-to-detector distance, we move the detector off the beam center. A one-dimensional plot generated from the collected x-ray diffraction pattern can then cover both small and wide angles, and processing of the two-dimensional pattern on the image requires only a simple definition of the beam center. Due to a significant reduction of the beam intensity at a low energy, the optimization of experimental conditions for collection of high quality images at short exposure times uses the following approach: the higher the x-ray energy, the smaller the beam stop and the shorter the sample-to-detector distance.

The key component in this scheme is the development of a four dimensional control system for our Mar345 detector. As shown in Fig.2, tracks attached to the B2 hutch roof are used to move the detector, effectively eliminating detector vibration during data collection. Buttons 2 and 3 control the movement of the detector horizontally, perpendicular and parallel to the beam, whereas knobs 4 and 5 control detector vertical position and rotation. At 25 keV, when the detector is ~450 mm from the sample, the small angle x-ray rings diffracted from a NP supercrystal are almost entirely blocked by the beam stop (Fig.2a). With x-ray energy tuned to 20 keV, the first-order small angle x-ray

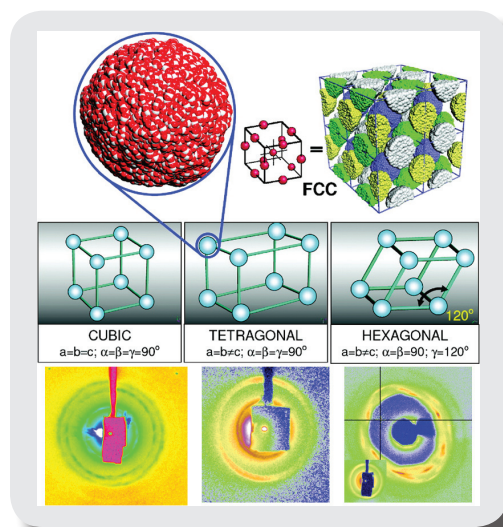


**Fig. 1:** Schematic illustrating the positioning of nanobuilding blocks into periodic crystallographic arrays and corresponding small angle x-ray diffraction patterns. Top left shows a spherical nanobuilding block, top right a superlattice comprising nanobuilding blocks located at face centred cubic (FCC) lattice points. Adapted partially from Ref [4].

diffraction rings are fully observable (Fig.2b), allowing refinement of the NP superstructure to BCT symmetry. In a FCC ordered supercrystal composed of slightly larger NPs, the full small angle x-ray diffraction pattern was observed by moving the detector distance to ~1200 mm.

Fig.3 shows one example of how well this technique worked for high pressure studies of NP supercrystals. By tuning the x-ray energy to several wavelengths at ambient conditions, the small angle and wide angle x-ray diffraction images of  $\text{In}_2\text{O}_3$  NP supercrystals<sup>8</sup> were collected and shown in Fig.3 (left). Small angle x-ray diffraction images (Figs.3a, 3b) confirm that 15 nm octahedral-shape NPs assemble into an ordered simple BCT superstructure. In addition,  $\text{In}_2\text{O}_3$  supercrystals display a noticeable lamellar structure that may be caused by a preferred orientation. Fig 3a was obtained using the small-angle setup at D1 with an energy of 10 keV and a sample to detector distance of 700 mm for comparison, and Fig 3b shows that our current set up at B2 can detect all SAXS rings with the exception of the first order.

The wide angle x-ray diffraction image and integrated pattern (Fig.3c) indicate that each single  $\text{In}_2\text{O}_3$  NP crystallizes into a cubic atomic structure. A pressure induced hexagonal phase has been observed at 10 GPa in bulk materials, but it does not appear in this NP supercrystal. However, small angle x-ray diffraction (Fig.3d) clearly reveals that the intermediate distance between NPs expands at pressures above 10 GPa. This

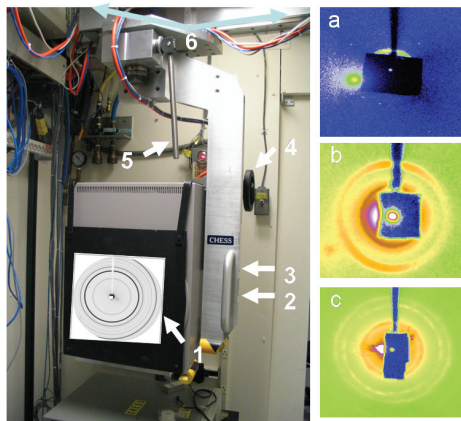


**Fig. 2:** (left) Four dimensional control of mar345 detector: 1) Mar345 Detector; 2) side-to-side (x); (3) Back-forward (y); (4) Vertical (z); (5) Rotation (x-y); (6) Moving tracks. (Right) small angle images of supercrystal with same particle size: a) 25 keV for BCT at short distance; b) 20 keV for BCT at long distance; c) 20 keV for FCC with slightly larger NPs at long distance.

enhanced structural stability could be attributed to combined effects of particle size, morphology and NP order; the pressure-induced expansion of inter-NP distance mostly results from a series of subtle surface structure variations. Additional examples have also been tested (Fig.1), and we observed several novel phenomena including: mechanical stability, phase transformation and associated changes in surface structure and nanoparticle interaction.

This unique capability opens a window for exploring new phenomena and tuning mechanisms for different NPs and NP building blocks under pressure. The collected information enables not only understanding the mechanical stability, multiple interactions, processes and resulting mechanism of nanoparticles

and packed building blocks [9], but also clarifying the development of surface properties upon pressure-induced phase transformation in single nanoparticles.

We appreciate technical assistance and discussions from all CHESS staff that made this high pressure technique feasible. Special thanks go to several collaborators including Prof. J. Fang (SUNY), Dr. H. Fan (SNL), Prof. D. C. Sayle (UK), Prof. T. Hyeon (Korea), Dr. R. Hoffmann (Cornell) for sample syntheses and valuable discussions.

## References:

1. M.A. Meyers, A. Mishra, and D.J. Benson; "Mechanical Properties of Nanocrystalline Materials", Prog. Mater. Sci. **51**, 427-556 (2006)
2. A.P. Alivisatos; "Semiconductor Clusters, Nanocrystals, and Quantum Dots", Science **271**, 933-937 (1996)
3. M.P. Pileni; "Self-assembly of Inorganic Nanocrystals: Fabrication and collective intrinsic properties", Acc. Chem. Res. **40**, 685-693 (2007)
4. D.C. Sayle, S. Seal, Z. Wang, et al; "Mapping Nanostructure: A systematic enumeration of nanomaterials by assembling nanobuilding blocks at crystallographic positions", ACS Nano **2**, 1237-1251 (2008)
5. B.D. Gates, Q.B. Xu, M. Stewart, et al; "New Approaches to Nanofabrication: molding, printing and other techniques", Chem. Rev. **105**, 1171-1196 (2005)
6. Y.N.Xia and G.M. Whitesides; "Soft Lithography", Ann. Rev. Mat. Sci. **28**, 153-184 (1998)
7. J. Aizenberg, J.C. Weaver, M.S. Thanawala, V.C. Sundar, D.E. Morse, and P. Fratzl; "Skeleton of Euplectella sp.: Structural hierarchy from the nanoscale to the macroscale", Science **309**, 275-278 (2005)
8. W.Q. Lu, Q.S. Liu, Z.Y. Sun, J.B. He, C. Ezeolu, and J.Y. Fang; "Supercrystal Structure of Octahedral  $c\text{-In}_2\text{O}_3$  Nanocrystals", J. Am. Chem. Soc. **130**, 6983-6991 (2008)
9. D.K. Smith, B. Goodfellow, D.M. Smilgies, and B.A. Korgel; "Self-assembled Simple Hexagonal  $\text{Ab}_2$  Binary Nanocrystal Superlattices; SEM, GISAXS and Defects", JACS, DOI: 10.1021/ja8085438, <http://pubs.acs.org/doi/abs/10.1021/ja8085438>

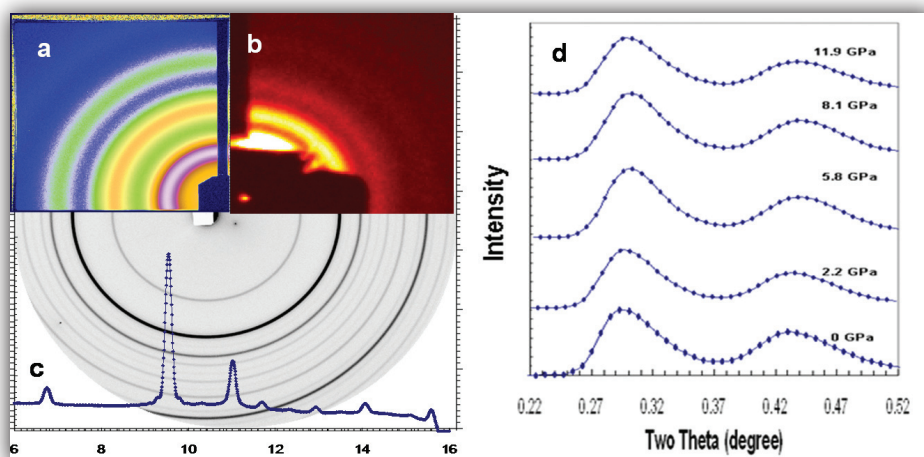


**Fig. 3:** Small and wide angle x-ray diffraction patterns of  $\text{In}_2\text{O}_3$  nanoparticle supercrystals at ambient and pressurized conditions. Panels a and b, small angle x-ray patterns at 0 pressure at different energies; c, wide angle x-ray image and integrated pattern; d, high pressure small angle x-ray scattering.